Table I. Vibrations Observed and Normal Coordinate Assignments[a] for Nickel(II) Porphyrin Schiff's Base Species

SB	SBH^+	assignment (no.)	SB	SBH^+	assignment (no.)
1652	1657	$B_{1g}(\nu_{10})$	1564		$E_u(\nu_{38})$
1639		$\nu_s(-N{=}CH-)$	1517	1518	$A_{1g}(\nu_3)$
	1650	$\nu_s(-{}^+NH{=}CH-)$	1378	1381	$A_{1g}(\nu_4)$
	1640	$\nu_s(-{}^+ND{=}CH-)$	1305	1306	$A_{2g}(\nu_{21})$
1598	1602	$A_{1g}(\nu_2)$		1154	$B_{2g}(\nu_{30})$
	1575	$B_{1g}(\nu_{11})$	1123	1122	$A_{2g}(\nu_{22})$

[a] Symmetries and mode numbers from Abe et al.[13] In the more correct C_{2h} group for 3 and 4, $\{A_{1g}, B_{1g}, A_{2g}, B_{2g}\}$ become A_g.

ranged from 0.1 to 0.75, consistent with the Franck-Condon scattering mechanism which dominates with Soret excitation.[12] Using the normal coordinate analysis of octaethylporphyrinato-Ni(II), we have collected several of the prominent vibrations of the Schiff's base species in Table I and assigned these in analogy with the results of Abe et al.[13] We have retained the D_{4h} symmetry notation characteristic of the porphyrin core. The Raman spectrum of **3** shows strong enhancement of totally symmetric modes at 1598 (ν_2), 1518 (ν_3), and 1383 cm^{-1} (ν_4). The line observed at 1652 cm^{-1} corresponds to a B_{1g} mode (ν_{10}), which is most likely enhanced through a Jahn-Teller or intramanifold coupling mechanism;[14] it is commonly observed when studying hemes and heme proteins by Soret excitation Raman.[15] The Schiff's base C=N stretching vibration is responsible for the line observed at 1639 cm^{-1}. We do not observe a clearly identifiable vinyl stretching mode. For the protonated Schiff's base, we note little change in the frequencies of the observed ring vibrations,[16] consistent with the NMR data above, which indicated that protonation effects are localized at the Schiff's base and do not strongly perturb the basic porphyrin bonding pattern. However, the decrease in symmetry, which is apparent in the optical spectrum, also appears to be reflected in the Raman spectrum of SBH^+ in that the scattered intensity from non-totally symmetric modes (B_{1g}, A_{2g}, B_{2g}) is stronger relative to the free Schiff's base.[17] Protonation of the Schiff's base shifts the N=C stretching frequency into the 1650-cm^{-1} region where it overlaps strongly with ν_{10}. In order to determine its frequency more precisely, we carried out analogous IR experiments that showed $\bar{\nu}(^+NH{=}CH) = 1650$ cm^{-1}; these data form the basis for the assignment of the two vibrational frequencies in Table I. If DCl is used to deuterate the porphyrin Schiff's base, the stretching frequency decreases to 1640 cm^{-1}. A similar pattern of -C=X- stretching vibration frequency shifts is observed in retinal Schiff's bases upon protonation and deuteration, and the physical mechanism underlying these shifts has been discussed in detail by Aton et al.[18] It appears as if the interaction between the C=N stretching vibration and the C=N-H bending mode is somewhat less in the porphyrin case than in the linear polyene retinal case.

The NMR and Raman data do not suggest an extensive π delocalization as the origin of the visible absorption spectral changes occurring in SBH^+, despite the apparent spectral similarities between **4** and the many well-characterized porphyrin π-cation radicals.[19] While the optical band shifts can result from a decrease in molecular symmetry, quantitative interpretation of the spectrum must await detailed MO calculations.

We speculated earlier[20] that a protonated Schiff's base linkage may be responsible for the unusual behavior of cytochrome *a*.[11] While the vibrational frequency of the Ni(II)-porphyrin $^+NH{=}CH-$ substituent is in reasonable agreement with that observed in oxidized cytochrome *a*, the optical spectrum of the protonated Schiff's base shows a significantly larger visible absorption red shift and Soret absorption band split than observed for the in situ chromophore. For this reason, it seems unlikely that a protonated Schiff's base is a good model for cytochrome *a*.[21] However, the unusual spectral properties of protonated metalloporphyrin Schiff's bases may have significant implications for other porphyrin-based systems. Photosynthetic systems provide a possible example in that chlorophyll absorption red shifts of the magnitude we report here are commonly observed in situ. These have sometimes been interpreted as resulting from dimer or higher order aggregate formation;[22] our results indicate that similar shifts can be obtained in a monomer system if protein/chromophore interactions occur.

Acknowledgment. This research was supported by grants from NIH (GM25480 to G.T.B.) and from NSF (to C.K.C.). C.K.C. is an Alfred P. Sloan Fellow (1980-1984) and a Camille and Henry Dreyfus Teacher-Scholar (1981-1985).

Registry No. 2, 84195-13-1; 3, 84195-14-2; **4**, 84195-15-3; butylamine, 109-73-9.

(11) Ondrias, M. R.; Babcock, G. T. *Biochem. Biophys. Res. Commun.* **1980**, *93*, 29-35.
(12) Felton, R. H.; Yu, N.-T. In "The Porphyrins"; Dolphin, D., Ed.; Academic Press: New York, 1978; Vol. III, pp 347-393.
(13) Abe, M.; Kitagawa, T.; Kyogoku, Y. *J. Chem. Phys.* **1978**, *69*, 4526-4534.
(14) Shelnutt, J. A. *J. Chem. Phys.* **1981**, *74*, 6644-6657.
(15) Callahan, P. M.; Babcock, G. T. *Biochemistry* **1981**, *20*, 952-958.
(16) The 3-4-cm^{-1} increases, which are apparent in ν_2 and in ν_{10} upon formation of the protonated Schiff's base, most likely arise from a slight porphyrin core contraction accompanying the protonation reaction.[15]
(17) The shifts observed in relative intensity for the symmetric and non-totally symmetric modes (D_{4h} notation) upon protonation of the Schiff's base may arise from symmetry reduction, which allows Franck-Condon enhancement of both classes of vibration. Alternatively, these shifts in intensity may arise from interference effects or changes in vibronic coupling introduced by the splitting observed in the optical absorption spectrum.
(18) Aton, B.; Doukas, A. G.; Narva, D.; Callender, R. H.; Dinur, U.; Honig, B. *Biophys. J.* **1980**, *29*, 79-94.
(19) Felton, R. H. In "The Porphyrins"; Dolphin, D., Ed.; Academic Press: New York, 1978; Vol. V, p 53.
(20) Babcock, G. T.; Callahan, P. M.; Ondrias, M. R.; Salmeen, I. *Biochemistry* **1981**, *20*, 959-966.
(21) In a separate series of experiments, however, we have found that a hydrogen-bond interaction between the formyl group of cytochrome *a* and a protein amino acid side chain provides an adequate explanation of the unusual properties of cytochrome *a* (Callahan, P. M.; Babcock, G. T. *Biochemistry*, in press).
(22) For a discussion of this point see: Davis, R. C.; Pearlstein, R. M. *Nature (London)* **1979**, *280*, 413-415.

Methylated Bases Stabilize Short RNA Duplexes

P. L. D'Andrea, D. Alkema, R. A. Bell,* J. M. Coddington, P. A. Hader, D. W. Hughes, and T. Neilson*

Departments of Biochemistry and Chemistry McMaster University, Hamilton, Ontario, Canada L8N 3Z5

Received August 9, 1982

The triribonucleotide GpCpA forms a stable duplex containing two G·C Watson-Crick base pairs and two 3'-dangling adenosines.[1,2] Dangling bases have been found to increase base stacking and thus improve overall duplex strength.[1-4] In this study, GpCpX sequences (where X = m^6A, m_2^6A, m^1G) were used as model systems to examine the effect of heterobase methylation on duplex stability (Figure 1). Results indicate that the stability of RNA duplexes

5'-GpCpX-3'
3'-XpCpG-5'

(1) Alkema, D.; Bell, R. A.; Hader, P. A.; Neilson, T. *J. Am. Chem. Soc.* **1981**, *103*, 2866-2868.
(2) Alkema, D.; Bell, R. A.; Hader, P. A.; Neilson, T. In "Biomolecular Stereodynamics"; Sarma, R. H., Ed.; Adenine Press: New York, 1981; pp 417-428.
(3) Martin, F. H.; Uhlenbeck, O. C.; Doty, P. *J.Mol. Biol.* **1971**, *57*, 201-215.
(4) Neilson, T.; Romaniuk, P. J.; Alkema, D.; Everett, J. R.; Hughes, D. W.; Bell, R. A. *Nucleic Acid Res. Spec. Publ.* **1980**, *no.* 7, 293-311.

0002-7863/83/1505-0636$01.50/0

Table I. ^{1}H NMR Chemical Shift Assignments for GCA over the Temperature Range 70–0 °C

	temperature, °C										
resonance	69.7	59.9	50.0	45.0	40.3	36.0	30.1	19.6	7.8	0.0	T_m, °C
AH-8	8.344	8.338	8.321	8.302	8.282	8.255	8.220	8.158	8.107	8.055	30.0
AH-2	8.185	8.159	8.108	8.061	8.007	7.944	7.861	7.720	7.621	7.541	32.6
GH-8	7.918	7.922	7.932	7.942	7.957	7.972	7.994	8.029	8.050	8.078	32.4
CH-6	7.701	7.696	7.687	7.678	7.671	7.663	7.654	7.640	7.630	7.626	39.3
AH-1′	6.059	6.054	6.048	6.042	6.039	6.035	6.031	6.024	6.014	6.000	NSB[a]
CH-1′	5.872	5.856	5.826	5.796	5.769	5.734	5.686	5.611	5.553	5.524	32.6
GH-1′	5.803	5.798	5.796	5.796	5.800	5.805	5.813	5.823	5.824	5.815	31.1
CH-5	5.827	5.781	5.706	5.645	5.583	5.515	5.431	5.304			37.8
											av 33.7

[a] NSB = no sigmoidal behavior.

Table II. ^{1}H NMR Chemical Shift Assignments for GCm^{6}A over the Temperature Range 70–0 °C

	temperature, °C										
resonance	69.7	59.9	50.0	45.0	40.3	36.0	30.1	19.6	7.8	0.0	T_m, °C
m^{6}AH-8	8.273	8.264	8.245	8.223	8.199	8.174	8.132	8.041	8.040	8.016	33.2
m^{6}AH-2	8.178	8.147	8.092	8.035	7.977	7.915	7.828	7.705	7.629	7.565	34.9
GH-8	7.905	7.908	7.923	7.938	7.955	7.976	8.002	8.082	8.069	8.079	33.2
CH-6	7.686	7.681	7.675	7.669	7.662	7.657	7.645	7.639	7.637	7.637	37.3
m^{6}AH-1′	6.051	6.045	6.041	6.036	6.033	6.032	6.023	6.024	6.022	6.018	NSB
CH-1′	5.855	5.838	5.808	5.778	5.744	5.706	5.645	5.573	5.515	5.515	32.9
GH-1′	5.785	5.780	5.782	5.786	5.793	5.801	5.811	5.820	5.827	5.822	34.3
CH-5	5.841	5.796	5.724	5.658	5.590	5.522	5.427	5.313	5.241	5.188	37.6
CH_3	3.026	3.012	2.993	2.976	2.960	2.944	2.919	2.882	2.850	2.838	33.8
											av 34.7

Table III. ^{1}H NMR Chemical Shift Assignments for GCm^{1}G over the Temperature Range 70–0 °C

	temperature, °C										
resonance	69.7	59.9	50.0	45.0	40.3	36.0	30.1	19.6	7.8	0.0	T_m, °C
m^{1}GH-8	7.946	7.935	7.898	7.863	7.823	7.782	7.731	7.661	7.613	7.582	36.4
GH-8	7.932	7.939	7.958	7.976	7.994	8.012	8.037	8.067	8.084	8.090	38.1
CH-6	7.704	7.697	7.683	7.672	7.661	7.652	7.643	7.634	7.632	7.631	45.7
CH-1′	5.880	5.861	5.822	5.784	5.748	5.715	5.672	5.622	5.594	5.583	39.9
m^{1}GH-1′	5.848	5.843	5.835	5.834	5.830	5.834	5.830	5.832	5.835	5.837	NSB
GH-1′	5.824	5.821	5.822	5.825	5.830	5.834	5.840	5.844	5.835	5.837	NSB
CH-5	5.844	5.793	5.690	5.610	5.531	5.458	5.368	5.264		5.170	40.8
CH_3	3.380	3.364	3.327	3.295	3.261	3.228	3.185	3.129	3.089	3.070	38.1
											av 39.8

Table IV. ^{1}H NMR Chemical Shift Assignments for GCm$^6_2$A over the Temperature Range 70–0 °C

	temperature, °C										
resonance	69.7	59.9	50.0	45.0	40.3	36.0	30.1	19.6	7.8	0.0	T_m, °C
m$^6_2$AH-8	8.232	8.222	8.197	8.175	8.153	8.135	8.109	8.036			41.9
m$^6_2$AH-2	8.095	8.055	7.975	7.909	7.844	7.788	7.713	7.602			41.4
GH-8	7.892	7.900	7.920	7.940	7.960	7.982	8.006	8.078			41.4
CH-6	7.683	7.679	7.668	7.658	7.647	7.639	7.626	7.611			39.1
m$^6_2$AH-1′	6.053	6.047	6.040	6.035	6.031	6.029	6.025	6.018			56.0[a]
CH-1′	5.844	5.825	5.783	5.745	5.702	5.662	5.609	5.534			38.0
GH-1′	5.761	5.758	5.762	5.767	5.772	5.778	5.778	5.771			43.8
CH-5	5.852	5.802	5.703	5.623	5.548	5.477	5.390	5.280			41.4
$(CH_3)_2$	3.303	3.286	3.257	3.237	3.218	3.201	3.183	3.161		3.323, 2.908	45.3
											av 41.5

[a] Not included.

increases in the order X = A < m^{6}A < m^{1}G < m$^6_2$A. Apparently, methylation of the 3′-dangling residue further enhances base stacking and duplex stability, with the site and degree of modification being significant factors. Similar results have been reported in optical studies of methylated adenosines in ribodinucleotides.[5,6]

A phosphotriester method was used to synthesize the required oligoribonucleotides.[7-9] Duplex formation was monitored by variable-temperature 400-MHz ^{1}H NMR spectroscopy and was discerned by examination of the sigmoidal curves generated on "chemical shift vs. temperature" graphs[10-12] (Tables I–IV, Figure 2). The average melting temperature[13] (i.e., T_m values) obtained

(5) Olsthoorn, C. S. M.; Haasnoot, C. A. G.; Altona, C. *Eur. J. Biochem.* **1980**, *106*, 85–95.
(6) Tazawa, I.; Koike, T.; Inoue, Y. *Eur. J. Biochem.* **1980**, *109*, 33–38.
(7) Gregoire, R. J.; Neilson, T. *Can. J. Chem.* **1978**, *56*, 487–490.
(8) Werstiuk, E. S.; Neilson, T. *Can. J. Chem.* **1976**, *54*, 2689–2696.
(9) England, T. E.; Neilson, T. *Can. J. Chem.* **1976**, *54*, 1714–1721.
(10) Alkema, D.; Hader, P. A.; Bell, R. A.; Neilson, T. *Biochemistry* **1982**, *21*, 2109–2117.
(11) Borer, P. N.; Kan, L. S.; Ts'O, P. O. P. *Biochemistry* **1975**, *14*, 4847–4863.
(12) Romaniuk, P. J.; Hughes, D. W.; Gregoire, R. J.; Bell, R. A.; Neilson, T. *Biochemistry* **1979**, *18*, 5109–5116.

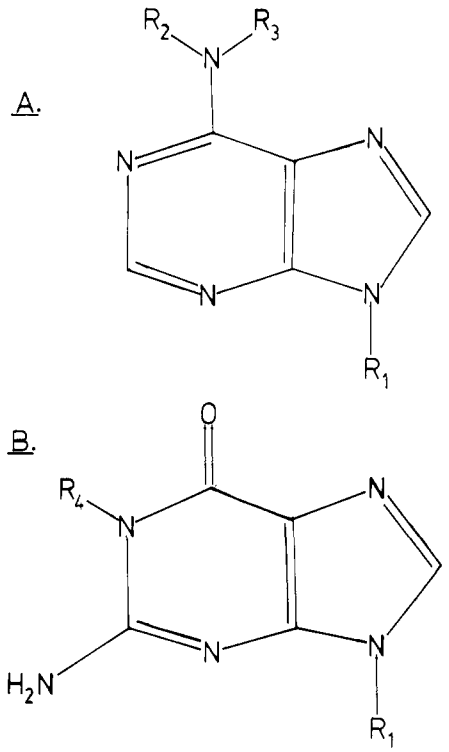

Figure 1. Methylated nucleosides used in trimer studies. N^6-methyladenosine (m^6A) R_1 = ribofuranoside, R_2 = H, R_3 = CH_3; N^6,N^6-dimethyladenosine (m_2^6A) R_1 = ribofuranoside, R_2 = R_3 = CH_3; N^1-methylguanosine (m^1G) R_1 = ribofuranoside, R_4 = CH_3.

at concentrations of 7.3 mM were as follows: GpCpA, 33.7; GpCpm^{6}A, 34.7; GpCpm^{1}G, 39.8; GpCpm$_2^6$A, 41.5 °C.

The upfield CH-5 chemical shift changes observed for all GpCpX:GpCpX duplexes indicated that normal G·C Watson–Crick base pairs were present.[1] The comparable upfield shifts noted for the XH-2 and XH-8 protons of the dangling methylated bases reflected 3′-nucleoside behavior similar to that of a 3′-dangling adenosine.[1]

The $J_{1',2'}$ coupling constants for the guanosine and cytidine residues in GpCpm^{6}A and GpCpm^{1}G were reduced to <0.5 Hz near 30 °C, while those for the 3′-dangling residues remained <1.0 Hz until 8 °C, as in the case of GpCpA. $J_{1',2'}$ values are indicative of the extent of base stacking;[14-16] thus in all instances, the guanosine and cytidine residues were fully stacked at temperatures at which the dangling residue retained some level of flexibility.[1,17] The comparative rate of $J_{1',2'}$ decline for the various XH-1′ protons parallels the relative order of duplex stability indicated by the T_m values.[1] The $J_{1',2'}$ values for the GpCpm$_2^6$A duplex decreased prior to those for corresponding protons in the other duplexes studied (i.e., below 40 °C for G and C and below 20 °C for m_2^6A). Clearly, the greater extent of methylation serves to facilitate duplex formation, probably due to increased hydrophobic interaction with the G·C core.

The chemical shift of the methyl groups in all three modified trimers experienced upfield sigmoidal changes with decreasing temperature, particularly in the case of GpCpm^{1}G, indicating increased methyl shielding during duplex formation.[1,4] Near 0 °C, two separate methyl resonances were observed for GpCpm$_2^6$A (δ 2.908 and 3.323). These signals reflected the generation of diastereotopic methyl groups as a result of restricted rotation about the N^6–C^6 bond.[18]

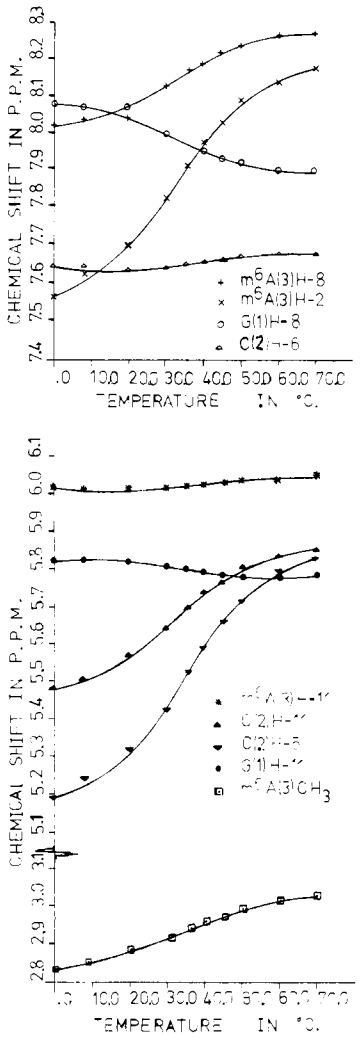

Figure 2. Chemical shift vs. temperature plots for GpCpm^{6}A at 7.3 mM. Samples were dissolved in 100% D_2O containing 0.01 M sodium phosphate buffer (pD 7.0) and 1.0 M sodium chloride.

The results presented here provide insight on the function of methylated nucleotides in native tRNA molecules. Examination of known tRNA sequences reveals frequent modification of bases immediately adjacent to the neck and anticodon regions.[19-21] Our present studies support the postulates (1) that methylated bases next to duplex regions contribute to the overall stability of tRNA molecules[19] and (2) that methylated bases contiguous to the anticodon 3′-terminus enhance mRNA–tRNA recognition, especially when the weaker A·U base pair occurs between the first position of the codon and the third position of the anticodon.

Acknowledgment. We thank the National Cancer Institute of Canada for financial assistance. The 400-MHz NMR spectra were obtained at the Southwestern Ontario NMR Center funded by a grant from NSERC.

Registry No. GpCpA, 5863-85-4; GpCpm^{6}A, 83967-63-9; GpCpm$_2^6$A, 83967-64-0; GpCpm^{1}G, 83967-65-1.

(13) Melting temperatures were determined by computer analysis using the minimum of the first derivative of a fifth-order equation, which is fitted to the chemical shift vs. temperature data.

(14) Romaniuk, P. J.; Neilson, T.; Hughes, D. W.; Bell, R. A. *Can. J. Chem.* **1978**, *56*, 2249–2251.

(15) Ezra, F. S.; Lee, C. H.; Kondo, N. S.; Danyluk, S. S.; Sarma, R. H. *Biochemistry* **1977**, *16*, 1977–1987.

(16) Altona, C. In "Structure and Conformation of Nucleic Acids and Protein-Nucleic Acid Interactions"; Sundaralingam, M., Rao, S. T., Eds.; University Park Press: Baltimore, 1975; pp 613–629.

(17) Cheng, D. M.; Danyluk, S. S.; Dhingra, M. M.; Ezra, F. S.; MacCross, M.; Mitra, C. K.; Sarma, R. H. *Biochemistry* **1980**, *19*, 2491–2497 and references therein.

(18) Van Charldorp, R.; Verhoeven, J. J.; Van Knippenberg, P. H.; Haasnoot, C. A. G.; Hilbers, C. W. *Nucleic Acids Res.* **1982**, *10*, 4237–4245.

(19) McCloskey, V. A.; Nishimura, S. *Acc. Chem. Res.* **1977**, *10*, 403–410.

(20) Cedergren, R. J.; Sankoff, D.; LaRue, B.; Grosjean, H. *CRC Crit. Rev. Biochem.* **1981**, *11*, 35–104.

(21) Gauss, D. H.; Sprinzl, M. *Nucleic Acids Res.* **1981**, *9*, r1–r23.